

# Role of the shape deformation in $^{12}\text{C} + ^{12}\text{C}$ fusion at sub-Coulomb energies

Le Hoang Chien, Bui Viet Anh, Thach Nguyen Ha Vy

**Abstract**—The fusion cross section of  $^{12}\text{C}+^{12}\text{C}$  system at the energies of astrophysical interest is calculated in the framework of barrier penetration model taking into account the deformed shape of interacting nuclei. In particular, the quadrupole surface deformation of both projectile and target nuclei has been included during the fusion process. The real and imaginary parts of nucleus-nucleus interactions performed using the Woods-Saxon square and Woods-Saxon functions, respectively have been carefully tested by  $^{12}\text{C}-^{12}\text{C}$  elastic scattering data analysis before employed to evaluate the astrophysical S factors (the fusion cross sections). The optical model results of elastic angular distributions are consistent with the experimental data. Within the barrier penetration model, the real part of the obtained optical potential gives a good description of the non-resonant astrophysical S factor. It turns out that the taking into account of quadrupole deformation of  $^{12}\text{C}$  nuclei increases the astrophysical S factor at energies below Coulomb barrier.

**Index Terms**—Barrier penetration model, deformation shape, fusion.

## 1 INTRODUCTION

Study of  $^{12}\text{C}+^{12}\text{C}$  fusion at low energies is important to understand the carbon burning stage in the massive stars (at least eight times of solar mass). In fact, after the helium burning phase, carbon nuclei are produced by the triple alpha processes. Due to gravitational collapse, the stars themselves increase their temperature to  $10^8$  K at which two  $^{12}\text{C}$  nuclei gain enough energy to fuse into each other and generate heavy elements such as  $^{20}\text{Ne}$ ,  $^{23}\text{Na}$ ,  $^{23}\text{Mg}$ . However, such typical condition in the stars corresponding to the thermal energy less than 1.5 MeV is not achieved in the experiments at the present time because the fusion cross section is estimated to be very small, in the order of  $10^{-10}$  mb. Moreover, in the energy region around and well below the Coulomb barrier, the prominent of resonant structures in  $^{12}\text{C}+^{12}\text{C}$  fusion excitation functions makes it extremely difficult to extrapolate the fusion cross section at energies of astrophysical interest from the available data at the higher energies [1]. Therefore, during the last four decades,  $^{12}\text{C}+^{12}\text{C}$  fusion at low energies still attracts a lot of experimental and theoretical efforts [2-12].

In general,  $^{12}\text{C}+^{12}\text{C}$  fusion cross sections at low energies are calculated using the barrier penetration model (BPM) [9, 10] that the reality strongly depends on the choice of nuclear potential. Indeed, a large number of potential models have been proposed to study  $^{12}\text{C}+^{12}\text{C}$  fusion based on both the microscopic and phenomenological approaches [9, 10, 12]. One could note that it is significant to determine how the potential model is good in the description of  $^{12}\text{C}-^{12}\text{C}$  nuclear interaction before employed to calculate the fusion cross section. However, the important step is rarely considered in previous

Received: 05-01-2018; Accepted 15-03-2018;  
Published: 15-10-2018.

Le Hoang Chien, Bui Viet Anh, Thach Nguyen Ha Vy,  
Faculty of Physics and Engineering Physics, University of  
Science, VNUHCM.

(e-mail: lhchien@hcmus.edu.vn).

studies [9, 10]. It is well known that the shape deformation of nuclei is important to the fusion at very low energies because the nucleus-nucleus interaction is sensitive to the orientation of incoming nuclei. As a result, the barrier heights performed from the nuclear and Coulomb potentials are expected to vary at various orientations of interacting nuclei. The various barrier height results in the changing of transmission coefficient that affects the fusion cross section. According to the experimental measurements, the ground state shape of  $^{12}\text{C}$  nuclei is well deformed [13]. Therefore, it is important to take into account the deformed shape of incoming nuclei in study of  $^{12}\text{C}+^{12}\text{C}$  fusion at low energies that previous studies have assumed the ground state shape of  $^{12}\text{C}$  nuclei to be spherical [9,12].

In this study, we focus on two important problems relevant to the  $^{12}\text{C}+^{12}\text{C}$  fusion at energies below the Coulomb barrier. Firstly,  $^{12}\text{C}-^{12}\text{C}$  nuclear potential at low energies performed using the Woods-Saxon square form has been carefully tested by the elastic scattering data analysis over a wide range of energies before applied into the BPM calculation. Secondly, the astrophysical S factors of  $^{12}\text{C}+^{12}\text{C}$  system are calculated in the framework of BPM taking into account the quadrupole surface deformation of  $^{12}\text{C}$  incoming nuclei.

In the next section, the outline of theoretical framework is described. Some calculated results of the nuclear potentials, elastic angular distributions and astrophysical S factors (fusion cross sections) of  $^{12}\text{C}+^{12}\text{C}$  system are given in the section of results and discussions. We summarize and conclude in the last section.

## 2 METHODS

### Optical Model

A large number of calculations successfully interpret the elastic scattering of nucleons and nuclei by nuclei have involved in term of the optical model (OM) analysis [14]. In the physical point of view, the OM describes the nuclei as cloudy balls which are heated by a beam of incoming particles, they partially absorb, scatter,

and transmit the beam in a way analogous to the behavior of light. To describe this assumption, the potential entered into the Schrodinger equation having a complex form (named optical potential) with the real and imaginary parts account for the elastic and non-elastic scattering processes, respectively. For detail derivation of OM formalism, one can see in [14]. In general, the differential cross section for the elastic scattering of an identical system is given in the form

$$\frac{d\sigma}{d\Omega_{el}} = \left| f_c(\theta) + f_c(\pi - \theta) + \frac{i}{k} \sum_{\ell = \text{even}} (2\ell + 1) \exp(2i\sigma_\ell) (1 - S_\ell) P_\ell(\cos(\theta)) \right|^2 \quad (1)$$

with  $k = \sqrt{2\mu E / \hbar^2}$  ( $\text{fm}^{-1}$ ). The Coulomb scattering amplitude  $f_c(\theta)$  is expressed in terms of the Coulomb phase shift  $\sigma_\ell$  and the Sommerfeld parameter  $\eta = 0.1574Z^2 \sqrt{\mu/E}$

$$f_c(\theta) = -\frac{\eta}{2k} \frac{\exp(-i\eta \ln[\sin^2(\theta/2)] + 2i\sigma_0)}{\sin^2(\theta/2)} \quad (2)$$

$S_\ell = \exp(2i\delta_\ell)$  is the nuclear scattering amplitude with the nuclear phase shift  $\delta_\ell$  determined by solving the Schrodinger equation

$$\left[ -\frac{\hbar^2}{2\mu} \frac{d^2}{dr^2} + U(r) + V_c(r) + \frac{\ell(\ell+1)\hbar^2}{2\mu r^2} - E \right] \chi(r) = 0. \quad (3)$$

$\mu$  is the reduced mass of  $^{12}\text{C}+^{12}\text{C}$  system (MeV).  $E$  is the center of mass energy (MeV) and  $\ell$  presents for the angular momentum between two colliding nuclei.  $U(r)$  is the optical potential (MeV) given in the form

$$U(r) = V_N(r) + iW_I(r). \quad (4)$$

The first and second terms of (4) correspond to the real and imaginary components of nuclear potential. The Coulomb potential  $V_c$  and Coulomb phase shift  $\sigma_\ell$  are taken the explicit formulas in [14].

### Barrier Penetration Model

In the framework of BPM [9,10], the fusion cross section induced by the collision of two

deformed nuclei could be averaged over all possible orientations of incoming nuclei as follows

$$\sigma_F = \frac{2\pi}{k^2} \sum_{\ell=\text{even}} (2\ell+1) \frac{1}{4} \times \int_0^\pi T_\ell(E, \theta_1, \theta_2) \sin \theta_1 d\theta_1 \int_0^\pi \sin \theta_2 d\theta_2. \quad (5)$$

Then, we use the useful treatment from the WKB approximation to evaluate the transmission coefficient given by

$$T_\ell(E, \theta_1, \theta_2) = \left[ 1 + \exp \left( \int_{r_1(E, \ell, \theta_1, \theta_2)}^{r_2(E, \ell, \theta_1, \theta_2)} t(r, E, \ell, \theta_1, \theta_2) dr \right) \right]^{-1},$$

$$t(r, E, \ell, \theta_1, \theta_2) = \sqrt{\frac{8\mu}{\hbar^2} |V(r, E, \ell, \theta_1, \theta_2) - E|}. \quad (6)$$

Here  $r_1, r_2$  are the classical turning points where  $V(r_1, E, \ell, \theta_1, \theta_2) = V(r_2, E, \ell, \theta_1, \theta_2) = E$ .

The effective potential  $V$  composing of the Coulomb, real part of nuclear and centrifugal interactions that depends on the angles  $(\theta_1, \theta_2)$ .  $\theta_1, \theta_2$  are the orientation angles of the projectile and target nuclei, respectively. The Coulomb interaction of two deformed nuclei is approximately calculated as follows [10]

$$V_C(r, \theta_1, \theta_2) = \frac{Z_1 Z_2 e^2}{r} \left\{ \frac{f_{12} \beta_{12} + f_{12} \beta_{22} + f_2 \beta_{12}^2}{+ f_2 \beta_{22}^2 + f_3 \beta_{12} \beta_{22} + 1} \right\}, \quad (7)$$

where,

$$f_{12}(r, \theta_i, R_{i0}) = \frac{3R_{i0}^2}{(2\ell+1)r^2} Y_{20}(\theta_i)$$

$$f_2(r, \theta_i, R_{i0}) = \frac{6\sqrt{5}R_{i0}^2}{3\sqrt{\pi}r^2} Y_{20}(\theta_i) \quad \text{with } i=1,2.$$

$$f_3(r, \theta_1, \theta_2, R_{10}, R_{20}) = \frac{R_{10}^2 R_{20}^2}{r^4} \left[ -\frac{3}{20\pi} + \frac{51}{25} Y_{20}(\theta_1) Y_{20}(\theta_2) + \frac{3}{10\sqrt{5}\pi} (Y_{20}(\theta_1) + Y_{20}(\theta_2)) \right]. \quad (8)$$

$R_{10}, R_{20}$  correspond to the spherical radius of projectile and target nuclei.  $\beta_{12}, \beta_{22}$  are quadrupole

deformation parameters of colliding nuclei, respectively.  $f_{12}, f_2, f_3$  are functions originated from multipole expansion of the Coulomb potential with respect to the orientation angles. The nuclear angle-dependent interaction can be assumed as [15]

$$V_N(r) = V_N^0(r) - (R_{10} \beta_{12} Y_{10} + R_{20} \beta_{22} Y_{20}) \frac{dV_N^0(r)}{dr}. \quad (9)$$

The superscript 0 in (9) presents for the spherical case of nuclear potential.

### 3 RESULTS AND DISCUSSIONS

#### $^{12}\text{C}+^{12}\text{C}$ Nuclear Potential

First, we search for the  $^{12}\text{C}-^{12}\text{C}$  realistic nuclear potential at low energies using the framework of OM calculations with the complex potential as described in (1)-(4). Seven elastic scattering angular distributions in laboratory energies between 1 and 6 MeV/nucleon, slightly above the Coulomb barrier [16], have been used in the searching the nuclear potential. The complex nuclear potential, as seen in (4), is assumed to have the phenomenological forms. The literature review of previous studies shows that the shallow potential has been often used to analysis the scattering data of  $^{12}\text{C}+^{12}\text{C}$  system at energies below 6 MeV/nucleon [17]. However, the family of deep potential has been considered as an appropriate choice to describe the experimental data in the higher energies [18, 19]. Based on the light of study in [18], the  $^{12}\text{C}-^{12}\text{C}$  potential at low energies could prefer to the deep type that is strong enough to keep two  $^{12}\text{C}$  nuclei in the cluster state of the compound  $^{24}\text{Mg}$  nucleus. Therefore, in this work, the real part of the complex nuclear potential at low energies is assumed to have a Woods-Saxon (WS) square shape that is the deep type and very similar to the shape of the microscopic folding potential [20]. The standard WS form is taken to describe the imaginary part. There are six adjustable parameters of  $V_0, R, a, W_0, R_I, a_I$ , as seen in (10), accounting for the central depth, reduced radius, and diffuseness of the real and imaginary nuclear potentials, respectively. These parameters are chosen to give the best description of elastic angular distribution data. In particular, each

elastic angular distribution is analyzed independently by varying these parameters to fit the experimental data. It means that at the minima six parameters correspond to the optimum potential with the shape and strength similar to the actual  $^{12}\text{C}-^{12}\text{C}$  nuclear interactions.

$$U(r) = \frac{V_0(E)}{\left[1 + \exp\left(\frac{r-R}{a}\right)\right]^2} + \frac{iW_0(E)}{1 + \exp\left(\frac{r-R_1}{a_1}\right)} \quad (10)$$

The comparison of elastic angular distributions obtained from the OM calculations with the experimental data in the energy range between 1 and 6 MeV/nucleon is shown in fig. 1 and fig. 2. One can see that the main structure of all angular distributions from the backward to forward angles is well reproduced with OM results using the potential parameters as listed in table I. The difference of differential cross sections at the minima and maxima between the calculated and measured results are reasonably accepted. One notes that the pattern of angular distributions at the backward angles is formed by the interference between the direct and reflected waves scattering in the interior region of potential while that at the forwards angles is originated from the interference of the waves incoming at the surface potential. It indicates that the nuclear potentials with parameters in table I have the reasonable depth and strength from the interior to surface that can be used to describe the actual  $^{12}\text{C}-^{12}\text{C}$  interaction at low energies.

**Table 1.** Parameters of the optical potential (10).

The volume integrals for the real ( $J_V$ ) and imaginary ( $J_W$ ) parts of nuclear potentials get the unit of  $\text{MeVfm}^3$

$E_{\text{lab}}$ (MeV)	$V_0$ (MeV)	$r$ (fm)	$a$ (fm)	$W_0$ (MeV)	$r_1$ (fm)	$a_1$ (fm)
16	372.0	0.751	1.421	2.241	1.468	0.218
	$J_V = 363$			$J_W = 18$		
18	370.0	0.751	1.421	2.442	1.418	0.260
	$J_V = 360$			$J_W = 17$		
20	367.0	0.751	1.421	2.866	1.431	0.215
	$J_V = 357$			$J_W = 21$		
35	363.0	0.753	1.426	2.399	1.574	0.202
	$J_V = 357$			$J_W = 24$		
40	260.0	0.752	1.426	3.069	1.486	0.201
	$J_V = 352$			$J_W = 26$		
45	365.0	0.755	1.428	3.427	1.426	0.232
	$J_V = 361$			$J_W = 25$		
50	357.0	0.755	1.428	4.479	1.403	0.333
	$J_V = 353$			$J_W = 30$		

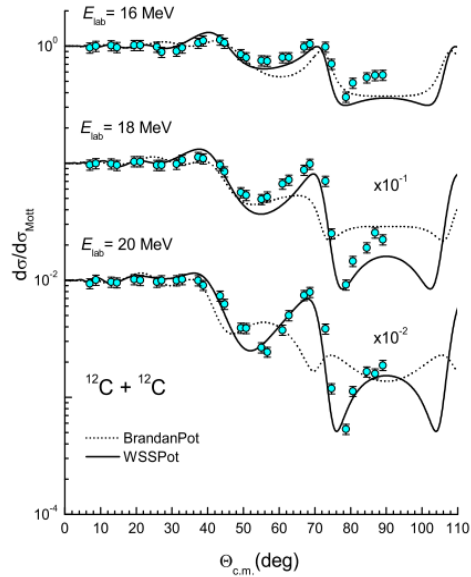


**Fig. 1.** The elastic angular distributions for  $^{12}\text{C} + ^{12}\text{C}$  system at the laboratory energies of 16, 18, 20 MeV. The solid lines and dotted lines account for the OM calculations using the potential model in this work and Brandan potential, respectively. The data are taken from [3].

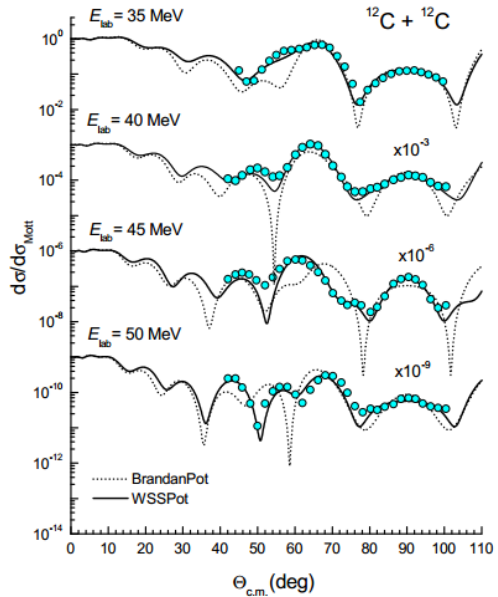


**Fig. 2.** The same as fig. 1 but for the laboratory energies of 30, 40, 45, 50 MeV [17]

For investigating whether the nuclear complex potentials performed in this work are unique or not, we calculate the volume integrals for the real ( $J_V$ ) and imaginary ( $J_W$ ) parts of nuclear potentials using the formula in [19] whose values are listed in table I. We make a comparison of the volume

integrals between the potential model in this work typical for low energies and the previous model giving a good description of the scattering data at higher energies. It is shown that there is a consistent continuation of the  $J_V$  and  $J_W$  values from the low energies to the higher energy region [19]. In the energy region below 6 MeV/nucleon, there are also some shallow and deep potential families [19] with the volume integrals  $J_V$  that is discrete with those of the potential family from higher energies. The discontinuity of volume integrals is ambiguous and unreasonable. Thus, we take a deep type potential of WS form ( $V_0=386.2-0.868E_{lab}$  (MeV),  $r=0.583$  (fm),  $a=0.902$  (fm),  $W_0=0.091E_{lab}$  (MeV),  $r_1=1.449$  (fm),  $a_1=0.318$  (fm)), one of mentioned discrete potentials named BrandanPot, as an example to analyze the  $^{12}\text{C}+^{12}\text{C}$  elastic scattering data, as seen in Fig. 1 and Fig. 2. The BrandanPot potential fails to describe the elastic angular distributions. Therefore, based on the elastic scattering analysis and the consistent continuation of volume integrals from high to low energies, it is reasonable to use the nuclear potential family obtained in this work to study the  $^{12}\text{C}+^{12}\text{C}$  fusion at low energies.

### $^{12}\text{C}+^{12}\text{C}$ fusion

In general, the astrophysical S factor that is the typical input for the fusion at energies of astrophysical interest is defined as a function of system energy and fusion cross section

$$S = E \sigma \exp(2\pi\eta). \quad (11)$$

where  $\sigma$  is calculated in the framework of BPM.

It is well known that the shape deformation of colliding nuclei is important to the sub-barrier fusion due to the dependence of the barrier high on the orientation of incoming nuclei [10]. The ground state shape of  $^{12}\text{C}$  nuclei is well deformed with the quadrupole and hexadecapole deformations obviously observed. In this work, we consider the effect of quadrupole deformation (correspond to  $\beta_2 = -0.40 \pm 0.02$  (fm)) [13] on  $^{12}\text{C}+^{12}\text{C}$  fusion at sub-Coulomb energies. To investigate the role of shape deformation in  $^{12}\text{C}+^{12}\text{C}$  fusion, we have constructed the deformed

Coulomb and nuclear potential corresponding to the case of two axial-symmetric nuclei, as described in (7) and (9).

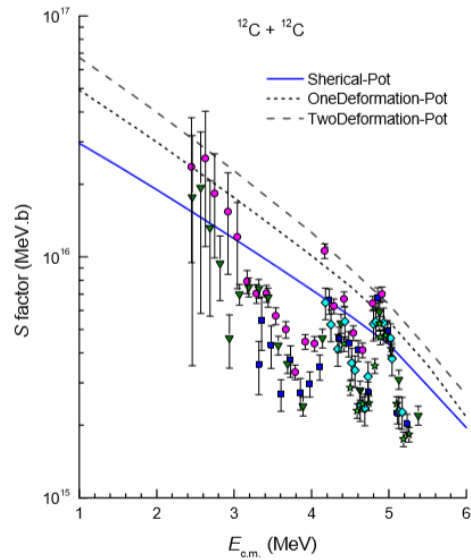


**Fig. 3.** Astrophysical S factor from  $^{12}\text{C}+^{12}\text{C}$  system at sub-Coulomb energies. Data are taken from Ref. [4-7].

The comparison between the calculated results of S factors from  $^{12}\text{C}+^{12}\text{C}$  fusion at energies below Coulomb barrier and the measured data [4-7] is illustrated in fig. 3. The solid line presents for the S factor calculated in the framework of BPM using the spherical potentials. The dotted line and dashed line describe the results in two approximations of one and two deformed nuclei, respectively. The data measured by various experimental groups are significantly different at energies below 5 MeV with strongly resonant peaks. However, the calculated results are consistent with most of the non-resonant data. One can see that the deformed effects on the astrophysical S factor are clearly obvious in the energy region below 5 MeV where is involved in the study of the fusion in star conditions while it can be negligible at the higher energies. The collision of quadrupole deformed target and spherical projectile produces higher astrophysical S factor in the order of 1.5 times than the spherical case. The simultaneous including of the quadrupole deformations in both target and projectile leads to the larger values of the astrophysical S factor. It is clear to indicate that

the role of deformed shape of colliding nuclei is not negligible in  $^{12}\text{C}+^{12}\text{C}$  fusion study.

#### 4 CONCLUSION

The OM and volume integral analyses show that the nuclear potential of  $^{12}\text{C}+^{12}\text{C}$  system at low energies prefer to the deep family consistently connecting to the potential family in higher energy region. The astrophysical S factors from  $^{12}\text{C}+^{12}\text{C}$  system calculated in the framework of BPM using the scattering potential with taking into account the quadrupole deformation of nuclear  $^{12}\text{C}$  surface agree well with the non-resonant data. Our calculations figure out that the account of the quadrupole deformation of  $^{12}\text{C}$  nuclei induces the increasing of the astrophysical S factor at sub-barrier energies. The including of surface deformation of  $^{12}\text{C}$  nuclei during the collision is important for the accurate calculation of the astrophysical S factor at the Gamow energies. The  $^{12}\text{C}$  nuclei has well deformed surface clearly dominated by not only the quadrupole but also the hexadecapole deformations. Therefore, the further calculation of  $^{12}\text{C}+^{12}\text{C}$  fusion at low energies should be done by taking into account both surface deformations of colliding nuclei.

#### TÀI LIỆU THAM KHẢO

- [1]. M.E. Bennett, R. Hirschi, M. Pignatari, S. Diehl, C. Fryer, F. Herwig, A. Hungerford, K. Nomoto, G. Rockefeller, F.X. Timmes, M. Wiescher, The effect of  $^{12}\text{C}+^{12}\text{C}$  rate uncertainties on the evolution and nucleosynthesis of massive stars, *MNRAS*, 420, 3047–3070, 2012, DOI: 10.1111/j.1365-2966.2012.20193.x.
- [2]. D.A. Bromley, J.A. Kuehner, E. Almquist, Resonant elastic scattering of  $^{12}\text{C}$  by carbon, *Phys. Rev. Lett.*, vol. 4, pp. 365–367, 1960, DOI: 10.1103/PhysRevLett.4.365.
- [3]. W. Treu, H. Frohlich, W. Galster, P. Duck, H. Voit, Total reaction cross section for  $^{12}\text{C}+^{12}\text{C}$  in the vicinity of the Coulomb barrier, *Phys. Rev. C*, 22, 2462–2464, Dec. 1980, DOI: 10.1103/PhysRevC.22.2462.
- [4]. J.R. Patterson, H. Winkler, C.S. Zaidins, Experimental investigation of the stellar nuclear reaction  $^{12}\text{C}+^{12}\text{C}$  at low energies, *ApJ.*, 157, 367–373, 1969, DOI: 10.1086/150073.
- [5]. M.G. Mazarakis and W.E. Stephens, Experimental measurements of the  $^{12}\text{C}+^{12}\text{C}$  nuclear reactions at low energies, *Phys. Rev. C*, 7, 1280–1287, 1973, DOI: 10.1103/PhysRevC.7.1280.
- [6]. E.F. Aguilera, P. Rosales, E. Martinez-Quiroz, G. Murillo, M. Fernández, H. Berdejo, D. Lizcano, A. Gómez-Camacho, R. Policroniades, A. Varela, E. Moreno, E. Chávez, M. E. Ortiz, A. Huerta, T. Belyaeva, and M. Wiescher, New  $\gamma$ -ray measurements for  $^{12}\text{C}+^{12}\text{C}$  sub-Coulomb fusion: Toward data unification, *Phys. Rev. C*, 73, 064601–1–12, 2006, DOI: 10.1103/PhysRevC.73.064601.
- [7]. M. Notani, H. Esbensen, X. Fang, B. Bucher, P. Davies, C.L. Jiang, L. Lamm, C.J. Lin, C. Ma, E. Martin, K.E. Rehm, W.P. Tan, S. Thomas, X.D. Tang, E. Brown, Correlation between the  $^{12}\text{C}+^{12}\text{C}$ ,  $^{12}\text{C}+^{13}\text{C}$ , and  $^{13}\text{C}+^{13}\text{C}$  fusion cross sections, *Phys. Rev. C*, 85, 014607–1–7, Jan. 2012, DOI: 10.1103/PhysRevC.85.014607.
- [8]. B. Bucher et al., “First Direct Measurement of  $^{12}\text{C}(^{12}\text{C},n)^{23}\text{Mg}$  at Stellar Energies”, *Phys. Rev. Lett.*, 114, 251102–1–6, 2015, DOI: 10.1103/PhysRevLett.114.251102.
- [9]. L.R. Gasques, A.V. Afanasjev, E.F. Aguilera, M. Beard, L.C. Chamon, P. Ring, M. Wiescher, and D.G. Yakovlev, Nuclear fusion in dense matter: Reaction rate and carbon burning, *Phys. Rev. C*, 72, 025806–1–14, 2005, DOI: 10.1103/PhysRevC.72.025806.
- [10]. V.Yu. Denisov, N. A. Pilipenko, Fusion of deformed nuclei:  $^{12}\text{C}+^{12}\text{C}$ , *Phys. Rev. C*, 81, 025805–1–5, 2010, DOI: 10.1103/PhysRevC.81.025805.
- [11]. C.L. Jiang, B.B. Back, H. Esbensen, R.V.F. Janssens, K.E. Rehm, R.J. Charity, Origin and consequences of  $^{12}\text{C}+^{12}\text{C}$  fusion resonances at deep sub-barrier energies, *Phys. Rev. Lett.*, 110, 072701–1–5, Feb. 2013, DOI: 10.1103/PhysRevLett.110.072701.
- [12]. M. Assunção, P. Descouvemont, Role of the Hoyle state in the  $^{12}\text{C}+^{12}\text{C}$  fusion, *Phys. Lett. B*, 723, 355–359, May 2013, DOI: 10.1016/j.physletb.2013.05.030.
- [13]. M. Yasue, T. Tanabe, F. Soga, J. Kokame, F. Shimokoshi, J. Kasagi, Y. Toba, Y. Kadota, T. Ohsawa, K. Furuno, Deformation parameter of  $^{12}\text{C}$  via  $^{12}\text{C}(\alpha,\alpha')$  and  $^{12}\text{C}(\alpha,\alpha'')$ , *Nucl. Phys. A*, 394, 29–38, 1983, DOI: 10.1016/0375-9474(83)90159-8.
- [14]. G.R. Satchler, Direct nuclear reactions, in *Clarendon Press*, Oxford, United Kingdom, 28, 1983.
- [15]. L.C. Chamon, G.P.A. Nobre, D. Pereira, E.S. Rossi, Jr., and C. P. Silva, Coulomb and nuclear potentials between deformed nuclei, *Phys. Rev. C*, 70, 014604–1–8, 2004, DOI: 10.1103/PhysRevC.70.014604.
- [16]. R.G. Stokstad, R.M. Wieland, G.R. Satchler, C.B. Fulmer, D.C. Hensley, S. Raman, L.D. Rickertsen, A.H. Snell, P.H. Stelson, Elastic and inelastic scattering of  $^{12}\text{C}$  by  $^{12}\text{C}$  from  $E_{\text{c.m.}} = 35\text{--}63$  MeV, *Phys. Rev. C*, 20, 655–669, 1979, DOI: 10.1103/PhysRevC.20.655.
- [17]. W. Reilly, R. Wieland, A. Gobbi, M. W. Sachs, J. Maher, R. H. Siemssen, D. Mingay, D.A. Bromley, Elastic-scattering excitation functions for the  $^{12}\text{C}\text{--}^{12}\text{C}$  system, *Nuovo Cimento*, 13, 913–922, 1973, DOI: 10.1007/BF02804158.
- [18]. Y. Kondo, M.E. Brandan, and G.R. Satchler, Shape resonances and deep optical potentials: A mean-field description of  $^{12}\text{C}+^{12}\text{C}$  scattering at low energies, *Nucl.*

- Phys. A*, 637, 175-200, 1998, DOI: 10.1016/S0375-9474(98)00212-7.
- [19]. M.E. Brandan, M. Rodríguez-Villafuente, A. Ayala,  $^{12}\text{C}+^{12}\text{C}$  elastic scattering analysis above  $E/A=6$  MeV using deep potentials, *Phys. Rev. C*, vol. 41, 1520–1529, 1990, DOI: 10.1103/PhysRevC.41.1520.
- [20]. Dao T. Khoa, G. R. Satchler, Generalized folding model for elastic and inelastic nucleus–nucleon scattering using realistic density dependent nucleon–nucleon interaction, *Nucl. Phys. A.*, 668, 3–41, 2000, DOI: 10.1016/S0375-9474(99)00680-6.

# Ảnh hưởng của biến dạng bề mặt hạt nhân lên phản ứng tổng hợp $^{12}\text{C}+^{12}\text{C}$ ở vùng năng lượng thấp

Lê Hoàng Chiến\*, Bùi Việt Anh, Thạch Nguyễn Hà Vy

Trường Đại học Khoa học Tự nhiên, ĐHQG-HCM

\*Tác giả liên hệ: lhchien@hcmus.edu.vn

Ngày nhận bản thảo: 05-01-2018, Ngày chấp nhận đăng: 15-3-2018, Ngày đăng: 15-10-2018.

**Tóm tắt**—Phản ứng tổng hợp  $^{12}\text{C}+^{12}\text{C}$  ở vùng năng lượng thiên văn được tính toán dựa trên mẫu xuyên rào lượng tử trong đó có kể đến ảnh hưởng của biến dạng bề mặt hạt nhân. Cụ thể, ảnh hưởng của biến dạng tứ cực lên tiết diện tổng hợp được khảo sát. Phần thực và ảo của thế tương tác hạt nhân được xây dựng lần lượt dựa trên dạng hàm Woods-Saxon bình phương và Woods-Saxon, đồng thời chúng được kiểm tra qua phân tích số liệu tán

xạ  $^{12}\text{C}-^{12}\text{C}$  ở vùng năng lượng gần ngưỡng Coulomb trước khi sử dụng trong các tính toán mẫu xuyên rào lượng tử. Kết quả tính toán của phân bố góc là phù hợp với dữ liệu thực nghiệm. Đồng thời, giá trị của hệ số thiên văn  $S$  trùng khớp với số liệu đo đạc trong trường hợp không cộng hưởng. Kết quả phân tích cho thấy việc kể đến biến dạng tứ cực của bề mặt hạt nhân  $^{12}\text{C}$  làm tăng tiết diện phản ứng tổng hợp ở vùng năng lượng dưới ngưỡng Coulomb.

**Từ khóa**—mô hình quang học, mẫu xuyên rào, phản ứng tổng hợp.